Japan Bilingual Publishing Co.

Transportation Development Research

https://ojs.bilpub.com/index.php/tdr

ARTICLE

Superelevation of Road Curves: Influence on Vehicles Fuel Consumption

Alex Coiret [1*] ***, Pierre-Olivier Vandanjon*** [2]

[1] *Structure et Instrumentation Intégrée (SII) Laboratory, Composants et Systèmes (COSYS) Department, Université Gustave Eiffel, 44340 Bouguenais, France*

[2] *Systèmes Productifs, Logistique, Organisation des Transports et Travail (SPLOTT) Laboratory, Aménagement, Mobilités et Environnement (AME) Department, Université Gustave Eiffel, 44340 Bouguenais, France*

ABSTRACT

Transport systems are primarily designed to address mobility and safety concerns. Today, energy consumption must also be taken into account in infrastructure design and operation, as environmental issues and tensions in oil production continue to intensify. For road transport, infrastructure requires energy for its construction, maintenance, and use. During the use phase, previous studies have assessed the influence of road texture, longitudinal slopes, and curvature on vehicle consumption. In this study, superelevation in curves is investigated as an additional parameter that may affect vehicle energy consumption. This investigation is first introduced using a simplified two-wheel model, showing a computed reduction in rolling resistance of 3% to 9% depending on cases. Full-scale experiments were then conducted using similar parameter ranges, with an instrumented passenger car on a curved road section featuring a continuous crossfall varying from 0 to 40%, and at three travel speeds: 80, 110, and 120 km/h. Experimental measurements confirm the numerical approach, with consumption reductions of up to 10% achieved for a light vehicle on a curve with optimal crossfall. The aim of this research is not to promote the design of all roads with high superelevation, which could be unsafe in most cases, but rather to contribute empirical knowledge to refine numerical consumption models. However, in specific situations such as high-speed highways, intermediate or high crossfall could be considered, provided that appropriate driver warnings are

*CORRESPONDING AUTHOR:

Alex Coiret, Structure et Instrumentation Intégrée (SII) Laboratory, Composants et Systèmes (COSYS) Department, Université Gustave Eiffel, 44340 Bouguenais, France; Email: alex.coiret@univ-eiffel.fr

ARTICLE INFO

Received: 24 December 2025 | Revised: 27 February 2026 | Accepted: 10 March 2026 | Published Online: 17 March 2026
DOI: https://doi.org/10.55121/tdr.v4i1.1052

CITATION

Coiret, A., Vandanjon, P.-O., 2026. Superelevation of Road Curves: Influence on Vehicles Fuel Consumption. Transportation Development Research. 4(1): 27–39. DOI: https://doi.org/10.55121/tdr.v4i1.1052

implemented or that advanced driving assistance systems become widespread. Future perspectives are discussed, taking into account other road requirements such as safety.

Keywords: Roads; Use Phase; Energy Consumption; Design; Crossfall; Vehicles

1. Introduction

Transport systems are mainly designed to ensure mobility and safety at a limited cost. Until now, research based on these criteria has contributed to improvements in road infrastructure: design rules generally focus on mobility and cost, resulting in choices regarding curvature radius and slopes [1], and safety is then evaluated, for example, using speed prediction models [2].

However, in general, this process is carried out regardless of the energy cost of infrastructure, despite the fact that roads have a considerable impact on anthropogenic climate change, representing 32% of global energy consumption in Europe [3] and even 81% of all transportation modes [4].

Some construction choices are driven by environmental considerations, such as the use of cold bituminous techniques, low-lime methods, and material recycling [5]. When considering medium- to long-term Life Cycle Analysis, use-phase energy costs exceed construction costs, even when accounting for time-related effects [6]. Some studies indicate that construction-phase energy is offset within a relatively short time [7, 8].

Road use-phase energy can be considered the sum of the fuel consumed by vehicles traveling on it. Reducing this consumption is relevant for fossil resource savings and climate change mitigation [9], since road transport cannot transition to renewable energy as easily as rail transport, which benefits from dedicated electrified infrastructure and high energy density systems.

Alternative road designs can lead to variations in use-phase energy consumption.

Slopes and speed limits are the most evident design and management parameters that significantly influence operation-phase energy consumption [10, 11]. Variations in vehicle speed or altitude induce significant changes in kinetic and potential energy, both of which increase with vehicle mass. Vehicle operating speeds depend on infrastructure design; thus, features such as roundabouts and intersections condition speeds, travel times, and eco-driving [12]. In particular, it has been demonstrated that good alignment between slopes and speed limits favors eco-driving [13] by reducing the need for mechanical braking when appropriate road design allows sufficient speed reduction without braking. However, as secondary design parameters, the influence of curvature radius and crossfalls on vehicle consumption has been scarcely investigated compared to longitudinal slopes [14, 15].

Even a complex model for consumption–travel time optimization [16], developed along an itinerary with speed planning as the optimization parameter, assumes a half-car model and no transverse slope. Research on electric vehicle consumption is usually more focused on vehicle weight and road longitudinal elevation profile and does not take into account the forces required to maintain vehicle speed and trajectory in curves, regardless of transverse slope [17]. Again, in the study by Gao et al. [18], speed limits are considered as a parameter for limiting vehicle consumption, with road input parameters such as longitudinal slope sequences, rolling resistance, and air resistance, but without considering radial forces in curves or transverse slopes. For longitudinal slope, a minimal value of 3% was identified as a critical threshold impacting vehicle consumption over a round trip.

Nevertheless, cornering losses have been assessed in the study by Dixon [19] as a function of mass, velocity, and radius. In Burgess and Choititle's study [20], it is pointed out that vehicle mass is the most significant parameter affecting energy demand, gravitational losses being proportional to it; again, cornering losses are found to increase with mass. Burgess and Choititle [20] report a cornering loss ratio of 6 for a mass ratio of 2.5 between the heaviest and lightest vehicles considered. Here, losses refer to the additional energy required to maintain vehicle speed and generate tire–road grip during a turning maneuver.

Practically, crossfalls are usually designed to ensure water runoff, and their maximum value is linked to the design speed [21]. Crossfall has also been studied in the railway context as a means of reducing contact stresses and rail wear [22, 23].

For a specific vehicle using magnetic levitation and running over a banked curvilinear path [24], relationships were

established between speed, superelevation angle, and lateral forces. The counterforce provided by superelevation allows cancellation of the centrifugal force associated with the turn. Simulations indicate an increase in allowable speed of approximately 7% for a 1° superelevation angle and about 56% for a 6° angle. This work shows that superelevation suppresses the need for lateral force to maintain a vehicle in a banked turn compared to a flat turn. These studies motivate the present research, which evaluates the influence of road superelevation on road vehicle energy consumption, particularly because this influence is often neglected, even for itineraries with numerous turns.

This work, focusing on vehicle consumption, concerns the operation phase of road infrastructures, regardless of other contributing phases such as construction and maintenance. The overall objective is to provide a general methodology for assessing road energy demand and to determine the influence of infrastructure geometry on construction, usage, and maintenance energy costs for optimization purposes. The work is experimentally and theoretically initiated in this paper for the less commonly studied parameter, crossfall, complementing ongoing research on longitudinal slopes [13].

2. Theoretical Energy Consumption in Curves

2.1. Study Context and Limitations

Road infrastructure geometry is determined to maximize both mobility and safety. This research focuses on evaluating an additional road function: energy efficiency. As discussed in the previous section, several studies have analyzed energy efficiency as a function of longitudinal slope, road texture, and speed limits, but crossfall in curves has not been considered as an influential parameter, except in railway numerical simulations [24]. This work aims to establish relationships between the superelevation angle in a curve and potential vehicle energy gains. The models and experiments are not limited to usual speeds or superelevation angles, since the objective is to determine the influence of crossfall rather than to propose design rules.

In straight sections, crossfalls induce transverse forces that vehicles must compensate for, thereby increasing energy consumption. In curves, however, this additional transverse force may facilitate the turning maneuver and thus reduce vehicle consumption. This work aims to evaluate this assumption.

Several constraints must be considered when analyzing banked curves:

- the minimum curvature radius must ensure sufficient grip for curve handling;
- the minimum crossfall must comply with surface water drainage requirements;
- the maximum crossfall must not endanger low-speed vehicles under low-grip conditions (when added centripetal forces exceed the combined centrifugal and tire grip forces).

The goal of the following subsection is to identify the physical origin of vehicle rolling resistance during cornering maneuvers. First, the phenomenon is introduced using a simplified model. Then, rolling resistance is assessed for curves with crossfall, with a large range of speeds and crossfall levels, beyond the classical values, to investigate the system limits.

2.2. Simplified Model of a Car in a Flat Curve

Rolling resistance expressions for a cornering maneuver can be found in vehicle dynamics reference books, such as Tires, Suspension, and Handling [19]. However, the assumptions underlying the mathematical expressions used are usually not fully explained. The following paragraphs bridge the gap between the usual equations for this relatively unknown rolling resistance and its physical origins.

The bicycle model (two-wheel vehicle model) is chosen to illustrate the characteristics of rolling resistance during a cornering maneuver. The name “bicycle model” comes from the fact that both wheels on the same axle are represented by an equivalent single wheel. This is a widely used model in vehicle dynamics [25]. Moreover, the system is assumed to be in a steady-state condition, i.e., the car moves at constant speed along a circular path of radius R.

Figure 1 presents a top view of the model. Although the angles shown in the figure are emphasized for clarity, the calculations are based on the small-angle approximation.

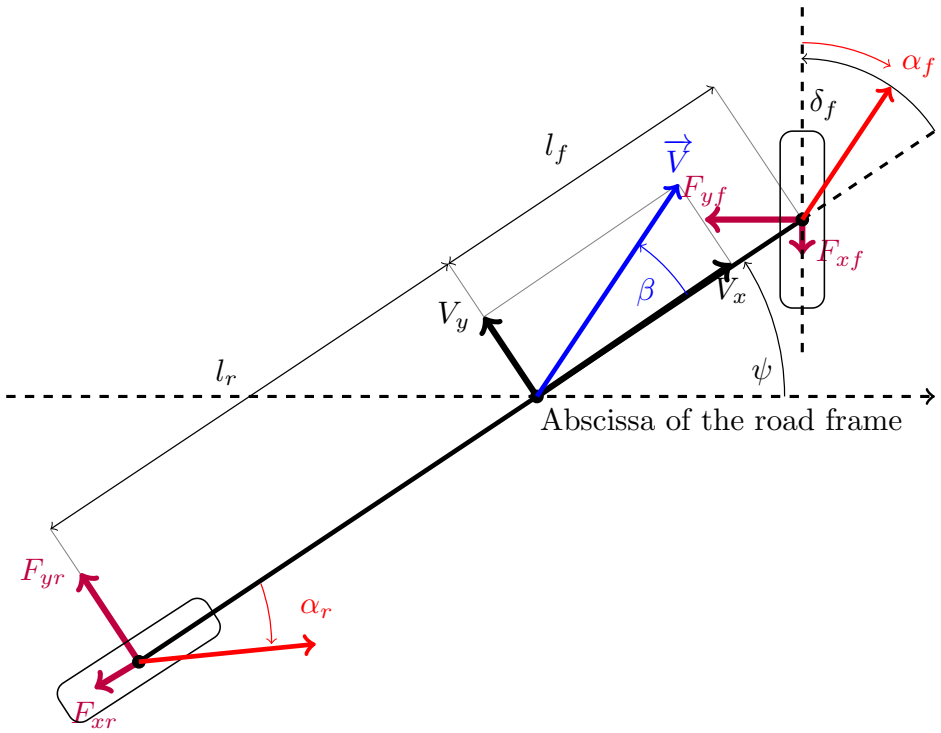

Figure 1. Two-wheels vehicle model in a cornering maneuver.

The variables are as follows: ψ is the yaw angle between the road reference frame abscissa and the vehicle longitudinal axis; β is the vehicle sideslip angle between the vehicle longitudinal axis and the gravity center velocity vector $\vec{V}$; α_f and α_r are the front and rear wheel sideslip angles; δ_f is the front steering angle, assumed identical for both front wheels. Assuming the vehicle is rigid, its velocity corresponds to the gravity center velocity, with longitudinal and transverse components v_x and v_y.

The geometric parameters are: vehicle mass m (kg); wheelbase l (m), equal to $l_f + l_r$, where l_f and l_r are the distances from the front and rear axles to the gravity center G. The vehicle travels at constant speed along a circular arc of radius R (m).

Kinematic rules allow to express α_i $(i = f, r)$ by δ_i, β, $\dot{\psi}$ and v_x:

$$\alpha_f = \beta + \frac{l_f \dot{\psi}}{v_x} - \delta_f \tag{1}$$

$$\alpha_r = \beta - \frac{l_r \dot{\psi}}{v_x} \tag{2}$$

In non-slip conditions, the lateral force F_y generated by the cornering maneuver and produced by tire–road grip counterbalances the centrifugal force $m\frac{V^2}{R}$.

Using the small-angle approximation, the simplified equation becomes:

$$F_y = F_{y_f} + F_{y_r} = \frac{mV^2}{R} \tag{3}$$

F_{y_f} and F_{y_r} are the front and rear transversal forces.

In steady driving conditions, a common assumption is a linear relationship between the sideslip angle and the lateral force through the tire cornering stiffness D_t (daN/°). As previously indicated, in this bicycle model, the right and left wheels of each axle are combined into equivalent mean wheels with common sideslip angles. Therefore, the cornering stiffness must be doubled,

$$F_{y_i} = 2D_{t_i}\alpha_i \tag{4}$$

with $i = f$ or r respectively for the front or rear tires.

The rolling resistance for a tire during a cornering maneuver is mainly related to two terms:

- energy dissipation due to bending of the sidewalls and tire–road contact. As a first approximation, this dissipation is assumed to be the same as in straight-line rolling;

- the work of the cornering force F_{y_i} in the direction of motion: $F_{y_i}\alpha_i$.

The total vehicle rolling resistance is the sum of each tire's rolling resistance. Thus, two phenomena are involved: energy dissipation in each tire and the specific projection of the front steering and rear wheel cornering forces.

The dissipation term can be approximated as $\mu_{rr} \cdot m \cdot g$, where μ_{rr} is the rolling resistance coefficient of the tires (speed dependent), and g is gravitational acceleration. μ_{rr} is considered here as a road-independent tire characteristic and assumed identical for all tires. This approximation could be refined by adding a term that varies with the speed, but it will not be worked out in order to be consistent with Dixon's equation.

The contribution specifically caused by the cornering maneuver, RR_c, is the sum:

$$RR_c = F_{yf}\alpha_f + F_{yr}\alpha_r. \tag{5}$$

This equation can be simplified.

Under the assumption $F_{yf} = F_{yr}$, Equation (3) becomes:

$$F_{yf} = F_{yr} = \frac{mV^2}{2R} = \frac{F_y}{2}. \tag{6}$$

By assuming that the cornering stiffness is the same for all the tires, Equation (6) associated with Equation (4) lead to:

$$\alpha_f = \alpha_r = \frac{mV^2}{4D_tR}. \tag{7}$$

By using this last result with the Equations (6) and (5), the part of the rolling resistance specifically caused by the curve, RR_c, can be assessed with the following formula:

$$RR_c = m^2\frac{V^4}{4D_tR^2} = \frac{F_y^2}{4D_t}. \tag{8}$$

RR_c has to be compared with the total drag of the car. In this purpose, the aerodynamic drag $\frac{1}{2}\rho C_x A_D V^2$ is computed with ρ the air density, A_D the drag area, C_x the drag coefficient. It is supposed that there is no surrounding wind in this simplified model. Then, the total resistance to the advancement in a curve, AR_c, can be approximated by:

$$AR_c = \mu_{rr}mg + \frac{1}{2}\rho C_x A_D V^2 + \frac{m^2V^4}{4D_tR^2}. \tag{9}$$

This equation, without the previous detailed argument, is presented in Dixon's book[19].

2.3. Banked Curve Model

The **Figure 2** displays a point-mass representation of a car on a curve with transverse slope angle θ. The vehicle is reduced to its center of gravity G; F_z is the normal road reaction force. In the presence of crossfall, the lateral force $F_{y_{CR}}$ equals the difference between the centrifugal force and the gravity component projected onto the road plane:

$$F_{y_{CR}} = m\frac{V^2}{R} - mg\theta = F_y - mg\theta. \tag{10}$$

F_y represents the lateral force required in the absence of crossfall to maintain the vehicle on the desired stable trajectory.

In a banked curve, this lateral force demand is reduced because part of the centrifugal force is compensated by the gravitational component acting along the inclined plane.

However, in extreme cases where the gravitational component exceeds the centrifugal force, the resulting lateral force becomes negative. This implies that a counteracting transverse force must be generated by the tires in the opposite direction to maintain the chosen trajectory.

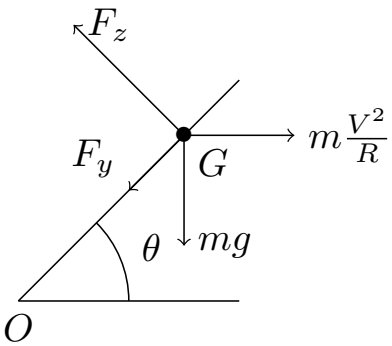

Figure 2. Balance of forces acting on a vehicle in a banked curve[19, 26].

In Equation (9), which expresses the total advancement resistance, the term $\frac{m^2V^4}{4D_tR^2}$ corresponds to the additional rolling resistance induced by cornering. In the presence of crossfall, this term becomes dependent on the effective lateral force $F_{y_{CR}}$, and can therefore be rewritten as $\frac{F_{y_{CR}}^2}{4D_t}$.

The reduction in lateral force leads to a quadratic reduction in cornering rolling resistance because of crossfall:

1. reduces the front and rear lateral forces (F_{yf} and F_{yr}) generated by tire–road contact;

2. reduces the sideslip angle α, which is proportional to these forces through the cornering stiffness.

From the rolling resistance Equation (9), and by taking into account the Equation (10), the rolling resistance in a banked curve is $RR_{c_{CR}}$:

$$RR_{c_{CR}} = m^2 \frac{(\frac{V^2}{R} - g\theta)^2}{4D_t}. \quad (11)$$

2.4. Numerical Application

The total advancement resistance in curve is computed for flat and banked configurations in this numerical application.

The common computation parameters are: the vehicle mass $m = 1,500$ kg, $D_t = 50,000$ N, the rolling resistance coefficient $C_{rr} = 0.01$, the aerodynamic parameters $C_x = 0.34$, $Ad = 2.25\,\mathrm{m}^2$, and the air density $\rho = 1.2\,\mathrm{kg/m}^3$.

In the case of the flat curve model, computation parameters are given in **Table 1**: speed of 90 km/h, radius equal to 400 m, lateral acceleration of 0.15 g, and crossfall equal to 0.

The numerical application becomes:

- The first term of rolling resistance is $\mu_{rr} mg = 147$ N,
- the sideslip angle is $0.7°$,
- the rolling resistance due to the bend is then $\frac{m^2 A^2}{4C_\alpha} = 27$ N,
- the aerodynamic drag is $\frac{1}{2}\rho V^2 A_D = 289$ N.
- leading to the total advancement resistance: $AR_c = 463$ N.

Table 1. Numerical computation of the total drag AR_c.

Maneuver	$\boldsymbol{R}$ **(m)**	$\boldsymbol{CR}$ **(°)**	$\boldsymbol{V}$ **(km/h)**	$\boldsymbol{AR_c}$ **(N)**
usual	400	0	90	463
usual	400	3	90	448
dedicated	314	6	110	622
dedicated	316	11	110	587
dedicated	318	17	110	572

In the case of banked curves, four crossfall angles and two vehicle speeds have been selected (Values given in **Table 1**).

For a small angle of $3°$, which is usual on open roads, the parameters and the resulting advancement resistance are given in the second line of **Table 1**. At this intermediate value, the influence of crossfall on rolling resistance is significant, since it reduces it by half, from 27 N to 12 N. The total advancement resistance becomes $AR_c = 448$ N. In this case, crossfall reduces the advancement resistance by 3%.

The last three lines of **Table 1** correspond to three dedicated experiments carried out on our test track, with a speed of 110 km/h and crossfall values of $10\%, 20\%$, and 30%. Overall, over this angle range, the total advancement resistance computed by the simplified model is reduced by 9%, from 622 N to 572 N.

2.5. Model Limits

Our model is simplified. In particular, it does not take into account the load transfer that occurs from the inside wheels to the outside wheels of a vehicle during a cornering maneuver. This transfer penalizes the grip potential of the inside wheels by reducing their vertical load. It alters the cornering stiffness and modifies the suspension geometry. Changes in suspension geometry affect wheel orientation and therefore modify the sideslip angle.

However, in a usual maneuver, these phenomena are mitigated by the crossfall effect, since crossfall itself reduces load transfer. In this case, load transfer has to counterbalance the resultant of both the centrifugal force and the gravity component projected onto the same plane. Conversely, the outside wheels benefit from an increased load and therefore from increased grip potential, assuming sufficient road surface quality and condition.

One assumption of the calculation is that energy dissipation due to the bending of the tire sidewalls is identical in straight-line and cornering conditions. It is clear that this term increases during a cornering maneuver because the sidewalls undergo greater deformation. However, this phenomenon is difficult to assess and depends on tire char-

acteristics. Crossfall, by reducing the sideslip angle and therefore tire deformation, decreases this dissipation.

In conclusion, our calculation is conservative regarding the influence of crossfall on advancement resistance. Despite this conservative assumption, the model indicates that a conventional crossfall reduces the total vehicle advancement resistance by 3%. Using a validated fuel consumption model (VTI report 748 A), the corresponding fuel consumption reduction is estimated at 1.5%.

This gain may appear modest, but it concerns the entire vehicle traffic. Consequently, cumulative individual gains could lead to significant energy savings. Moreover, it is consistent with improved road safety, since transverse grip is less demanded to maintain the curved trajectory.

These results are difficult to assess under normal driving conditions because of various sources of disturbance arising from poorly controlled parameters, such as weather conditions (wind field, air density, temperature) or vehicle state (engine and tire temperatures, vehicle wear). Dedicated experiments were therefore designed to assess the influence of selected crossfall levels.

For this purpose, the simplified bicycle model is used to verify whether the conditions of our dedicated experiments allow quantification of the role of crossfall in energy consumption.

These results are subject to some uncertainties, related to load transfer effects (with both benefits and drawbacks), as well as to non-linearities and small-angle approximations.

Although subject to discussion, these results suggest that the influence of crossfall can be detected experimentally, which constitutes the objective of this theoretical section: to forecast and estimate the results of the subsequent experimental phase of this work.

3. Experimental Evaluation of Crossfall Influence

3.1. Experimental Setup

Full-scale tests have been carried out with an instrumented passenger car on a circular test track, with the aim of identifying consumption variations under different crossfall levels. The specific test track presents several crossfall levels for almost the same curvature radius (**Figure 3**).

Figure 3. Test vehicle on the C_2 crossfall level trajectory.

The test vehicle, a RENAULT CLIO, is a medium-sized passenger car equipped with numerous instruments, the most important for this study being a Kistler dynamometric wheel mounted on the right front wheel, a Correvit optical speedometer, a wind speed anemometer on the roof, an inertial measurement unit, and proprietary sensors whose data are delivered via the vehicle CAN bus (instantaneous fuel consumption, steering wheel angle, …). Data are acquired at a common sampling frequency of 100 Hz.

The portion of the test track used in this study is a cir-

cular curve approximately 1,100 m long, with a progressive crossfall from 0% to 41%, for a proportional radius ranging from 312 to 320 m. For the study requirements, five crossfall levels are considered, named C_1 to C_5, and associated with the following (crossfall level, radius) pairs: C_1 (0,312); C_2 (10,314); C_3 (20,316); C_4 (30,318); and C_5 (41,320).

Each test consists of a run along the whole curve at a stabilized speed and steering angle. Tests are performed at speeds of 80, 110, and 120 km/h, and for three different crossfall levels at each speed (indeed, some combinations of speed and crossfall levels lead to abrupt and strong control inputs, which are not pursued in this context; therefore, only 3 out of the 5 crossfall levels have been operated for each speed case).

Main recorded data are:

- vehicle speed determined optically by means of a Correvit;
- longitudinal and transversal relative wind speeds measured 20 cm above the vehicle roof by means of two axial anemometers;
- instantaneous fuel consumption acquired from the vehicle CAN bus;
- longitudinal and transverse contact forces for the right front wheel measured by means of a Kistler dynamometric wheel;
- applied torque to this wheel measured by means of strain gauges fitted on the transmission arm;
- vehicle yaw rate extracted from the inertial measurement unit.

3.2. Experimental Results

Some recorded data from a particular test case are plotted in **Figure 4**, corresponding to the lowest speed and lowest crossfall level case, i.e., the 80 km/h and flat crossfall test case.

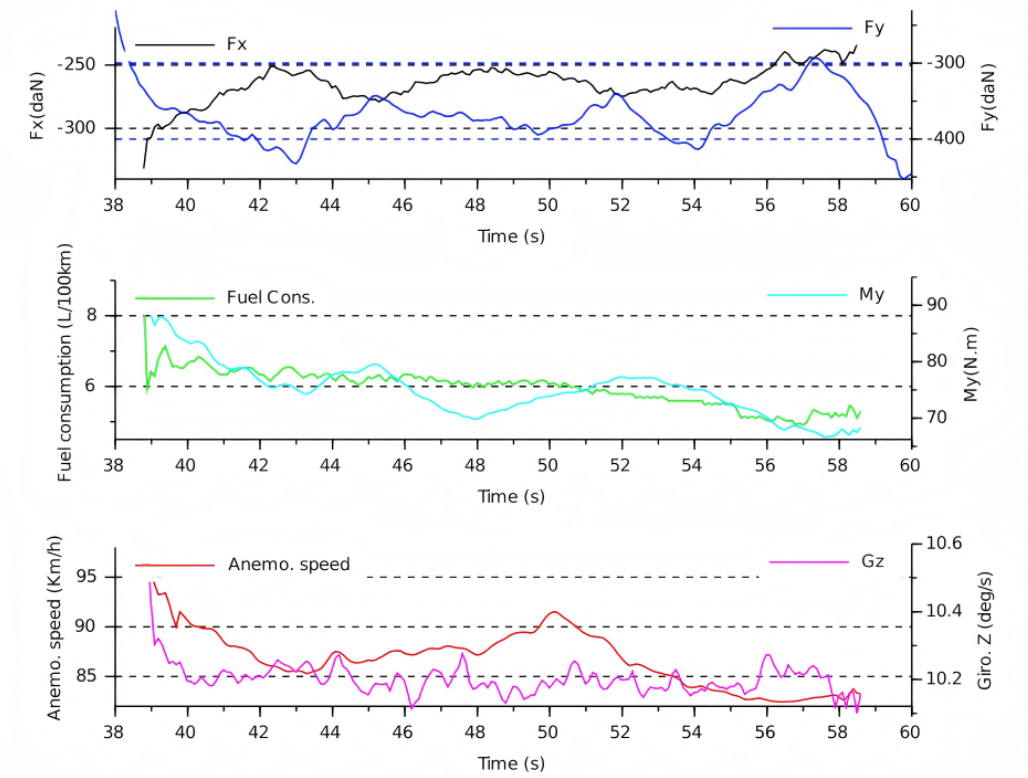

Figure 4. Stationary test run filtered signal data.

Note: Test conditions: 80 km/h speed and C_1 crossfall level.

Experimental data are acquired at a frequency of 100 Hz over a total duration of about 15 s, starting a few seconds after reaching a steady state in vehicle dynamics. The plotted data result from two successive numerical treatments: the data are first smoothed by means of a linear centred averaging function and then decimated by means of a block-to-point

averaging function in order to reduce the number of retained values.

It can be noted that the plotted data in **Figure 4** correspond to a longer duration than the retained data. Nevertheless, noticeable signal variations are due to engine instability, wind fluctuations, and unavoidable driver-related factors.

For the sensitivity study of the crossfall parameter, global mean values are used for each experimental case. Mean values of the most significant measured parameters are given in **Tables 2–4** for all tested situations.

In the particular case of the low speed of 80 km/h (**Table 2** and **Figure 4**), for which the crossfall level is greater than necessary to balance the low centrifugal forces, fuel consumption is reduced by 2.5% and 5% with successive increases in crossfall from C_1. The assumption of transversal force compensation by the gravity component is nevertheless not fulfilled. Indeed, the negative F_y force for the C_1 crossfall case corresponds to the natural behaviour in which the driver must generate a centripetal force when driving through a curve. For the C_2 and C_3 crossfall cases, the crossfall levels are too high and positive F_y forces must be generated to remain on the chosen stable path. In other words, an outward force must be applied by the driver to avoid an oversteering manoeuvre. For these two latter cases, in the tangential plane of the road, the gravity component becomes higher than the dynamically induced centrifugal forces, and the difference must be compensated by tire lateral forces.

For the speed of 110 km/h, the measurements given in **Table 3** are consistent with the anticipated result that the required transversal driving force F_y decreases with increasing crossfall level, since the gravitational component in the road plane partly compensates for the centrifugal forces due to curve dynamics. This decrease in required transversal contact force is confirmed by a reduction in steering angle. Although fuel consumption is not uniquely and directly dependent on these two indicators, it decreases significantly for the C_3 and C_4 situations compared with the C_2 test case, by 5.4% and 10.3%, respectively.

Table 2. Lower speed test case (80 km/h): Fuel consumptions, contact forces and steering angle for the three experimented crossfall values C_1 to C_3.

Test Case	Speed (km/h)	Cons. (l/100)	F_x (N)	F_y (N)	Steer (°)
80 km/h, C_1	77.4	5.96	-264	-369	-17.1
80 km/h, C_2	77.2	5.81	-231	262	-10.7
80 km/h, C_3	77.3	5.67	-225	457	-8.5

Table 3. Intermediate speed test case (110 km/h): Fuel consumptions, contact forces and steering angle for the three experimented crossfall values C_2 to C_4.

Test Case	Speed (km/h)	Cons. (l/100)	F_x (N)	F_y (N)	Steer (°)
110 km/h, C_2	106.4	7.55	-351	-436	-15.8
110 km/h, C_3	106.4	7.14	-336	-157	-13.6
110 km/h, C_4	106.4	6.77	-343	-123	-13.2

In this speed case, gravity compensation of the transversal force is never excessive; that is to say, the speed/crossfall combinations for the C_3 and C_4 levels both constitute improvements compared with the speed/C_2 crossfall combination.

It goes without saying that this improvement in fuel consumption for the C_2 to C_4 crossfall cases at 110 km/h is fully dependent on the vehicle class. The improvement is observed here for a passenger car, but it could differ for a heavy vehicle. The present work aims to emphasize the achievable energy savings within a given test framework.

At last, for the highest tested speed of 120 km/h, the measurements given in **Table 4** exhibit the same behaviour of successive decreases in steering angle and transversal contact force for the right front wheel with increasing crossfall level from C_3 to C_5. Meanwhile, reductions in fuel consumption are observed but are not proportional to the crossfall increase, with 7% and 4.3% reductions for the C_4 and C_5 levels, respectively, compared with the C_3 fuel consumption level.

Table 4. Highest speed test case (120 km/h): Fuel consumptions, contact forces and steering angle for the 3 experimented crossfall values C_3 to C_5.

Test Case	Speed (km/h)	Cons. (l/100)	F_x (N)	F_y (N)	Steer (°)
120 km/h, C_3	116.2	8.54	-390	-626	-17.6
120 km/h, C_4	116.2	7.94	-397	-468	-15.4
120 km/h, C_5	116.1	8.17	-386	-225	-12.8

A careful review of the recorded data leads to the conclusion that measurements on the right front wheel cannot be assimilated to a two-wheel model at such high crossfall levels as C_4 and C_5. Further experiments should therefore include force measurements on both front wheels to account for transverse load transfers. Indeed, despite lower effective fuel consumption for higher crossfall levels, the longitudinal force F_x varies only slightly, particularly because these crossfalls above 20% generate significant load transfer and force asymmetry.

The **Figure 5** shows the overall reductions in fuel consumption for the three test speeds over five subplots corresponding to the five crossfall levels. This synthesis figure confirms significant fuel reduction with increasing crossfall, except for the previously discussed case at the highest speed and highest crossfall level.

Despite the limited number of crossfall levels tested, a near-linear relationship between crossfall and fuel consumption is observed for two out of the three speed cases, as highlighted by dashed lines in **Figure 5**.

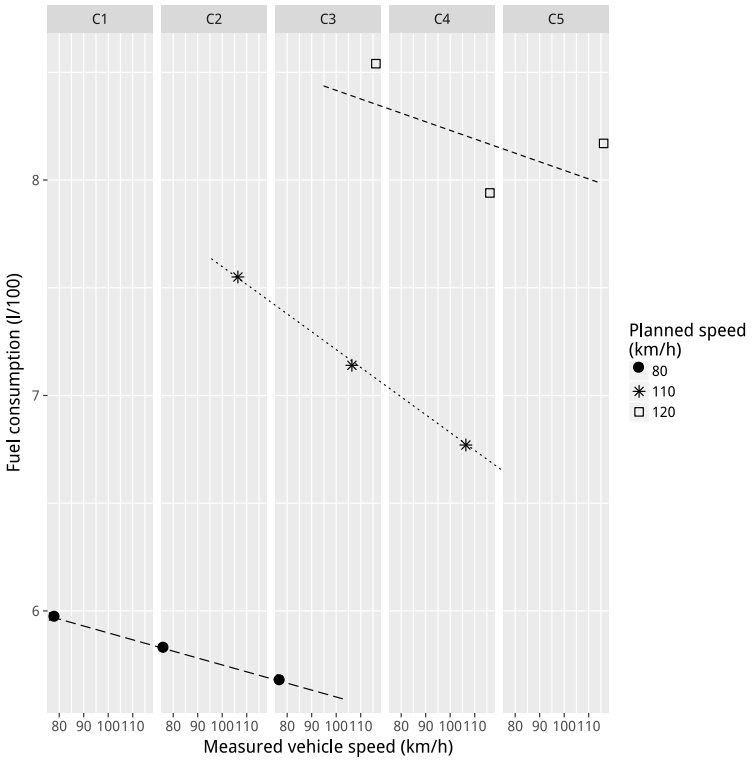

Figure 5. Fuel consumptions vs. crossfall cases and test speeds.

4. Discussion

The literature provides many elements for modeling vehicle fuel consumption on straight roads and longitudinal slopes, but very few investigations address the influence of curves and banked curves on fuel consumption. Aside from classical fuel consumption parameters such as vehicle characteristics, wind field fluctuations, driving inputs, road materials, and slopes, this work aims to propose a first experimental assessment of crossfall in curves.

The full-scale experiments show that in the case of a crossfall level that is excessive relative to the operating speed of the vehicle, a transversal force must be developed in a direction opposite to that required in the flat crossfall situation. This phenomenon is induced by the excessive gravity component, which overcomes the centrifugal component in the road plane. It represents a real drawback of banked curves, since it results in a non-natural and unexpected manoeuvre for a driver travelling at too low a speed. This situation was encountered for the 80 km/h speed case with significant crossfall. Despite this, fuel consumption reductions between 2.5% and 5% were observed for this low-speed case, for the C_2 and C_3 crossfall configurations compared with the flat curve C_1 configuration.

For the same light vehicle, experiments carried out at higher speeds of 110 km/h and 120 km/h do not lead to the same drawback. In these cases, the crossfall does not appear to be excessive, since the transversal force decreases without changing sign. The gravitational force contributes to reducing the transversal forces, as predicted by Equation (10). Consequently, it also contributes to a reduction in the wheel steering angle, which is a secondary efficiency indicator of crossfall influence.

Reductions in fuel consumption appear to be significant, ranging from about 5.4% to 10.3% at the intermediate speed of 110 km/h and from 4.3% to 7% at the highest speed of 120 km/h.

The intermediate speed case can be considered the most appropriate combination of crossfall selection, vehicle speed, and vehicle mass in terms of fuel consumption optimization.

On the other hand, the higher speed case shows limitations in force evaluation from measurements, due to the limitations of a two-wheel model and the use of a single instrumented wheel. Furthermore, such high crossfall levels are not considered by vehicle manufacturers, and components such as suspensions are not operating within their normal use range.

This experimental work was conducted over a wide range of crossfall values, at moderate and high speeds, and for a single passenger car. The objective was not to investigate high crossfall levels from a road design perspective, but rather to explore a broad experimental range of this geometric parameter, since almost no previous experimental research had been conducted in this area.

It appears that high crossfall levels can be difficult for drivers to handle at low speeds. At high speeds, the limitations arise more from vehicle characteristics, as vehicles are not designed for such specific infrastructure conditions.

Nevertheless, at a typical speed of 80 km/h, intermediate crossfall levels, slightly higher than conventional ones, can lead to fuel consumption reductions of 2.5% to 5% compared with the flat curve case. Moreover, the transversal forces required to maintain the vehicle trajectory are lower, resulting in reduced use of road grip potential and potentially improved overall safety.

These results should be considered as part of an experimental study, with possible practical applications limited to moderate crossfall values adapted to usual operating speeds. Finally, this research should be extended to include experiments with heavy vehicles, utility vehicles, and motorbikes.

5. Conclusion

Mid-term expectations regarding oil availability, oil prices, and climate change justify new investments in transport systems to improve their energy efficiency.

In this context, reducing the energy demand of the road transportation system is a key objective for fossil resource savings, since road transport is less likely than rail transportation, for example, to shift entirely to renewable energy sources.

Without altering safety or mobility standards, alternative road designs can lead to variations in operational phase fuel consumption. While slopes and speed limits have already been studied with this objective, the influence of curvature radius and crossfall on vehicle consumption has been scarcely investigated, although cornering losses have been assessed as a function of mass, velocity, and radius.

In this work, the influence of crossfall in curves has first been evaluated theoretically using a simplified two-wheel model and then assessed experimentally.

Full-scale tests have been carried out with an instrumented passenger car on a circular test track approximately 1,100 m long, with a progressive crossfall from 0% to 41%, corresponding to radii ranging from 312 to 320 m. Five crossfall levels have been considered within this range for the study.

Experimental results have shown that when the cross-

fall level is excessive relative to the vehicle operating speed, a transversal force must be developed in a direction opposite to that required in the flat crossfall case, with the gravity component not only assisting in reducing the centrifugal component but actually overcoming it in the road plane. Such excessive crossfall should be avoided, as it implies non-natural and potentially unsafe manoeuvres. Despite this drawback, fuel consumption reductions of up to 5% have been achieved in the low-speed case of 80 km/h for relatively high crossfall levels of 10% and 20%.

An intermediate speed case of 110 km/h appears to be the most appropriate combination of crossfall selection, vehicle speed, and vehicle mass in terms of fuel consumption optimization. Fuel consumption reductions of 5.4% and 10.3% have been achieved for crossfall levels of 20% and 30%, respectively, compared with the reference level of 10%. In this experiment, the flat curve case was not recorded because it would have required excessively high transversal forces on the tires.

For the higher speed case of 120 km/h, fuel consumption reductions ranging from 4.3% to 7% have been observed. However, force measurements were less conclusive, as the assumption of vehicle symmetry could no longer be considered valid for crossfall levels greater than 20%, and therefore two instrumented wheels would be required. Moreover, vehicles are not designed for such conditions, and mechanical failures could occur in components such as the suspension.

In this initial stage, a simple symmetrical model has been established and used to facilitate the experimental evaluation. The experiments demonstrate the potential of crossfall variations to reduce vehicle fuel consumption on curved road sections within a reasonable range of crossfall values, particularly at relatively high speeds.

In future work, a broader range of experimental conditions is planned, particularly for different types of vehicles such as heavy vehicles, buses, or motorbikes, and with a more finely discretized set of crossfall levels.

Author Contributions

Conceptualization, A.C. and P.-O.V.; methodology, A.C. and P.-O.V.; data curation, A.C. and P.-O.V.; writing—original draft preparation, A.C. and P.-O.V.; writing—review and editing, A.C. and P.-O.V. Both authors have read and agreed to the published version of the manuscript.

Funding

This work received no external funding.

Institutional Review Board Statement

Not applicable.

Informed Consent Statement

Not applicable.

Data Availability Statement

All relevant data are to be found in the preceding Tables.

Conflicts of Interest

The authors declare no conflict of interest.

References

[1] SETRA, 2000. ICTAAL: Instruction on the Technical Conditions for the Development of Connecting Highways. SETRA: Bagneux, France. pp. 1–58. Available from: https://dtrf.cerema.fr/pdf/pj/Dtrf/0002/Dtrf-0002540/DT2540.pdf (in French)

[2] Esposito, T., Mauro, R., Russo, F., et al., 2011. Speed prediction models for sustainable road safety management. Procedia Social and Behavioral Sciences. 20, 568–576.

[3] Baptista, P.C., Silva, C.M., Farias, T.L., et al., 2012. Energy and environmental impacts of alternative pathways for the Portuguese road transportation sector. Energy Policy. 51, 802–815.

[4] Monzon, A., Sobrino, N., Hernandez, S., 2012. Energy- and Environmentally Efficient Road Management: The Case of the Spanish Motorway Network. Procedia - Social and Behavioral Sciences. 48, 287–296.

[5] Blanc, J., Hornych, P., Sotoodeh-Nia, Z., et al., 2019. Full-scale validation of bio-recycled asphalt mixtures for road pavements. Journal of Cleaner Production. 227, 1068–1078.

[6] Jiang, R., Wu, P., 2019. Estimation of environmental impacts of roads through life cycle assessment: A critical review and future directions. Transportation Research Part D: Transport and Environment. 77,

148–163.

[7] Araújo, J.P.C., Oliveira, J.R., Silva, H.M., 2014. The importance of the use phase on the LCA of environmentally friendly solutions for asphalt road pavements. Transportation Research Part D: Transport and Environment. 32, 97–110.

[8] Stripple, H., 2001. Life Cycle Assessment of Road; A Pilot Study for Inventory Analysis. IVL Swedish Environmental Research Institute: Stockholm, Sweden.

[9] Mukhopadhyay, K., Forssell, O., 2005. An empirical investigation of air pollution from fossil fuel combustion and its impact on health in India during 1973–1974 to 1996–1997. Ecological Economics. 55(2), 235–250.

[10] Coiret, A., Vandanjon, P.O., Bosquet, R., et al., 2012. Energy consumption induced by operation phase of railways and road infrastructures. In Proceedings of the 2nd International Conference on Road and Rail Infrastructure, Dubrovnik, Croatia, 7–9 May 2012.

[11] Roumegoux, J.-P., 1995. Calcul des émissions unitaires de polluants des véhicules utilitaires. Science of The Total Environment. 169(1–3), 205–211.

[12] Ciarla, V., Chasse, A., Moulin, P., et al., 2016. Compute Optimal Travel Duration in Eco-Driving applications. IFAC-PapersOnLine. 49(11), 519–524.

[13] Coiret, A., Vandanjon, P.O., Cuervo, A.T., 2016. Eco-driving potentiality assessment of road infrastructures according to the adequacy between infrastructure slopes and speeds limits. In Proceedings of the 4th International Conference on Road and Rail Infrastructure (CETRA 2016), Sibenik, Croatia, 23–25 May 2016; pp. 589–595.

[14] Kang, M.W., Shariat, S., Jha, M.K., 2013. New highway geometric design methods for minimizing vehicular fuel consumption and improving safety. Transportation Research Part C: Emerging Technologies. 31, 99–111.

[15] Sentoff, K., Aultman-Hall, L., Holmén B., 2015. Implications of driving style and road grade for accurate vehicle activity data and emissions estimates. Transportation Research Part D: Transport and Environment. 35, 175–188.

[16] Consolini, L., Laurini, M., Locatelli, M., 2026. A convex reformulation for speed planning of a vehicle under the travel time and energy consumption objectives. Automatica. 185, 112811. DOI: https://doi.org/10.1016/j.automatica.2025.112811

[17] Song, J., 2025. Evaluation of driving resistance and energy consumption in electric vehicles under various ambient and tire temperatures using real-world driving data. ETransportation. 25, 100454. DOI: https://doi.org/10.1016/j.etran.2025.100454

[18] Gao, C., Xu, J., Jia, M., et al., 2024. Correlation between carbon emissions, fuel consumption of vehicles and speed limit on expressway. Journal of Traffic and Transportation Engineering (English Edition). 11, 631–642. DOI: https://doi.org/10.1016/j.jtte.2023.02.007

[19] Dixon, J.C., 1996. Tires, Suspension, and Handling, 2nd ed. Society of Automotive Engineers: Warrendale, PA, USA; Arnold: London, UK.

[20] Burgess, S.C., Choititle, J.M.J., 2003. A parametric study of the energy demands of car transportation: A case study of two competing commuter routes in the UK. Transportation Research Part D: Transport and Environment. 8(1), 21–36.

[21] Kang, M.W., Jha, M.K., Schonfeld, P., 2012. Applicability of highway alignment optimization models. Transportation Research Part C: Emerging Technologies. 21(1), 257–286.

[22] Jin, X., Xiao, X., Wen, Z., et al., 2009. An investigation into the effect of train curving on wear and contact stresses of wheel and rail. Tribology International. 42(3), 475–490.

[23] Wang, J., Chen, X., Li, X., et al., 2015. Influence of heavy haul railway curve parameters on rail wear. Engineering Failure Analysis. 57, 511–520.

[24] De Angelo, M., D'Ovidio, G., 2021. Lateral displacement evaluation for a high-Temperature superconducting magnetic levitation experimental vehicle running over a banked curvilinear path. Physica C: Superconductivity and Its Applications. 591, 1353974.

[25] Vandanjon, P.-O., Coiret, A., Lorino, T., 2014. Application of viability theory for road vehicle active safety during cornering manoeuvres. Vehicle System Dynamics. 52(2), 244–260.

[26] Orfila, O., Coiret, A., Do, M.T., et al., 2010. Modeling of dynamic vehicle–road interactions for safety-related road evaluation. Accident Analysis and Prevention. 42, 1736–1743.